Functional Materials Letters
Vol. 16, No. 2 (2023) 2350010 (4 pages)

DOI: 10.1142/S1793604723500108

World Scientific
www.worldscientific.com

Flexible strain sensor with self-healing function for human motion monitoring

Shanpeng Ji*, Ping Guo*, Diqing Ruan*, Huaping Wu†, Lin Cheng* and Aiping Liu*,‡

*Key Laboratory of Optical Field Manipulation of Zhejiang Province
Zhejiang Sci-Tech University, Hangzhou 310018, P. R. China
†Key Laboratory of Special Purpose Equipment and Advanced Processing Technology
Ministry of Education and Zhejiang Province, College of Mechanical Engineering
Zhejiang University of Technology, Hangzhou 310023, P. R. China
‡liuaiping1979@gmail.com

Received 7 February 2023; Revised 25 February 2023; Accepted 17 March 2023; Published 21 April 2023

Flexible strain sensors with highly similar effects to human skin have been given great attention due to their potential application in personal health monitoring, human–computer interaction systems and artificial electronic skin fields. In particular, the self-healing properties of the sensors are important for their long-term and repeated use during the actual operation. Herein, a flexible strain sensor with complete self-healing function is proposed by combining self-healable PDMS film with rich hydrogen bonds and conductive ink based on recoverable liquid metal. By adjusting the contents of different components of self-healing PDMS film and the relative mass fraction of the liquid metal ink in the strain sensor, the tensile stress and resistance of flexible sensor can be changed to match different usage scenarios. The sensor can achieve a maximum tensile stress of 0.83 MPa and an elongation at break of 843%. After self-healing for 24 h at room temperature, its tensile stress can revert to 82% of the original value, while the electrical connection can instantaneously recover to initial situation after fracture surface contacts. This hints its potential advantage as wearable sensors for motion monitoring of the human body and developable applications in medical monitoring, recyclable electronics and artificial skin.

Keywords: Self-healing; flexible sensor; strain sensing; motion monitoring.

Flexible sensing technology is developing rapidly with the innovation of sensing material and processing technology. Compared with traditional rigid sensors, flexible sensors have good flexibility[1] and dexterity.[2–4] In addition, flexible sensors have lower fabrication costs and high wearability, which make them widely used in human–computer interaction,[5–7] medical monitoring,[8] environmental protection,[9] wearable devices,[10] etc. Furthermore, flexible sensors should also have the same inherent self-healing capability just like human skin in order to recover their sensing capability after damage.

To date, many scientists have designed stable and durable self-healing sensors by utilizing various strategies, and the main research has focused on self-healing hydrogels.[11] However, hydrogels cannot meet the needs of good mechanical properties and long-term stability due to their own drawbacks, which are fatal for flexible sensors. Some scientists have also introduced dynamic covalent bonds and supramolecular interactions as crosslinking sites in polydimethylsiloxanes (PDMSs) polymer,[12,13] as they can be reversibly broken and reformed, leading to repetitive self-healing characteristics. Although many self-healing polymers with excellent properties (high tensile properties, robust mechanical capabilities, good fracture tolerance, etc.) have been widely reported,[14,15] the self-healing materials with satisfactory sensing functions remain a key issue to be addressed to realize their practical applications in the flexible skin sensor. Usually, a second conductive network is introduced into the self-healing material, but this affects the self-healing properties of the material, and the sensing capability of this composite material tends to decrease after the material suffers multiple damages because its sensing part does not have self-healing properties.[16,17] Therefore, how to prepare a material with excellent mechanical property, self-healing function and the ability to recover electrical sensing signals is a problem that needs to be solved.

In this paper, a self-healable PDMS film with rich hydrogen bonding (H-PDMS) is prepared by a one-pot method, and a recoverable ink is prepared using liquid metal. These two elements can be well integrated to form a flexible self-healing sensor with a layer-by-layer structure (Fig. 1). The sensor has good self-healing capacities in both mechanical and electrical properties and presents long-term sensing stability. This simple and scalable strategy can be applied to develop self-healing materials for electronic devices application, such

‡Corresponding author.

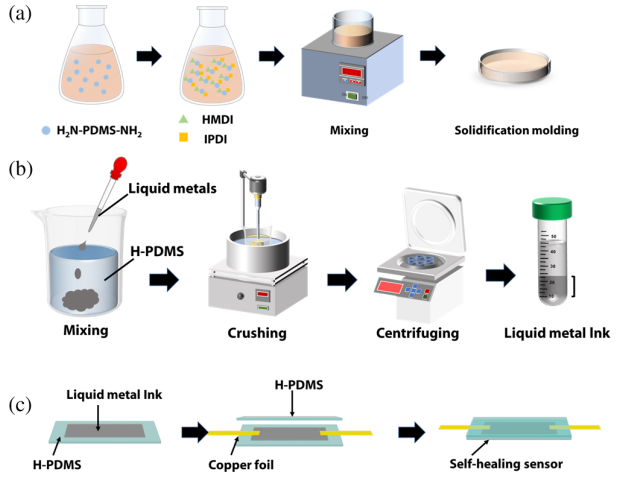

Fig. 1. Preparation processes of (a) H-PDMS film, (b) liquid metal ink and (c) monolithic flexible sensor with sandwich structure.

as wearable sensor, health monitoring and human–computer interaction system.

The preparation process of self-healing H-PDMS film was shown in Fig. 1(a). Different molar ratios of 4,4′-methylenebis (cyclohexyl isocyanate) (HMDI) and isophorone diisocyanate (IPDI) (2:8, 4:6, 6:4 and 8:2) were added into the bis(3-aminopropyl) terminated poly(dimethylsiloxane) (H_2N–PDMS–NH_2), thus forming H-PDMS polymer film after curing and molding, and the samples were defined as H-PDMS$_{0.2}$, H-PDMS$_{0.4}$, H-PDMS$_{0.6}$ and H-PDMS$_{0.8}$, respectively, and were cut into long strips (25 mm × 10 mm × 0.5 mm) for use as substrates. The H-PDMS solution containing some liquid metal Ga75.5%/In24.5% (5–40 wt.%) was crushed using a cell crusher and centrifuged to obtain a self-healable liquid metal ink (Fig. 1(b)). The ink containing H-PDMS could be well integrated with the substrate material. Then conductive copper foils were contacted with liquid metal ink and encapsulated by another piece of H-PDMS film to form a monolithic flexible sensor with sandwich structure (Fig. 1(c)).

The Fourier transform infrared (FTIR) spectra of the H-PDMS were obtained on an FTIR spectrophotometer in the range from 4000 cm^{-1} to 500 cm^{-1}. UV–Vis absorption spectroscopy was performed in the range from 400 nm to 1000 nm to characterize the optical properties of materials. X-ray photoelectron spectroscopy (XPS) was employed to determine the states of C and O elements in the H-PDMS. The surface roughness of the material was measured with a laser confocal microscope. The structure of liquid metal ink was analyzed with a scanning electron microscope (SEM). The contact angle of a material was measured at a temperature of 25°C in ambient conditions. The mechanical parameters of self-healing sensor (25 mm × 10 mm × 1 mm) were examined using a mechanical testing machine with a loading speed of 30 mm/min. The electrical characteristics of sensors were evaluated by a Keithley 2400 digital source meter and sampled at a rate of 0.1 s. All self-healing tests were conducted at room temperature without external interference.

Figure S1(a) shows the infrared spectra of PDMS and H-PDMS. The typical peaks of urea amide I and amide II between 1500 cm^{-1} and 1700 cm^{-1} prove the successful preparation of H-PDMS.[18–20] In addition, the amide II band of the polymer can be found between 1565 cm^{-1} and 1570 cm^{-1}, which is a typical peak of hydrogen bonding system. The SEM image of liquid metal ink in Fig. S1(b) shows that the liquid metal dispersed in the H-PDMS presents spheres of up to 1 μm in diameter and remains stable. The distance between liquid metal spheres can be adjusted by stretching, controlling the resistance and sensing behavior of the sensor. When the synthesized H-PDMS was kept at 25°C and 60°C for 24 h, respectively, C1s and O1s core level spectra of XPS, UV–Vis absorption spectra, surface roughnesses and water contact angles of H-PDMS reserved at the two temperatures were compared. The results indicate that the physical properties of H-PDMS are almost unchanged (Figs. S2 and S3), verifying the good stability of synthesized H-PDMS at use temperature below 60°C. Moreover, the H-PDMS stored at either 25°C or 60°C does not conduct electricity.

In the H-PDMS preparation, HMDI and IPDI provide different crosslinking sites for PDMS, respectively, and their molar ratios will affect the mechanical properties of self-healing sensors. Figures 2(a) and 2(b) demonstrate the maximum tensile lengths as well as tensile stresses of self-healing sensor with different molar ratios of HMDI/IPDI. With the HMDI content increase in H-PDMS, the stress at fracture of the sensor increases because HMDI with symmetric structure can form relatively strong hydrogen bonds with anti-HMDI in a synergistic manner to provide good mechanical properties, while IPDI usually forms weaker hydrogen bonds for

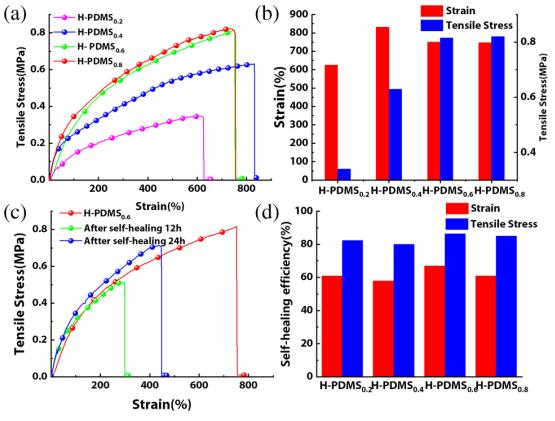

Fig. 2. (a) Stress–strain curves of flexible sensors prepared with different composition contents, (b) corresponding maximum stress and strain, (c) stress–strain curves of flexible sensors (H-PDMS$_{0.6}$) after self-healing at room temperature for 12 h and 24 h and (d) self-healing efficiency of flexible sensors after self-healing at room temperature for 24 h.

energy dissipation,[21] allowing H-PDMS to maintain a more stable film. By this strategy, the modulus of H-PDMS is easily adjusted to accommodate different parts of the skin, and the maximum stress can reach 0.83 MPa. At the same time, the tensile deformation rate reaches 600%, far exceeding the maximum deformation rate of human skin (approximately 60%), satisfying the need for a flexible sensor. When the sensors is cut-off and cured at room temperature for 12 h and 24 h, the maximum stress of healable sensors recovers to about 80% of original ones when the sensors self-heal at room temperature for 24 h, while the maximum tensile amount could recover to 60% of the original one (Figs. 2(c) and 2(d)). This is due to the fact that the prepared H-PDMS possesses a large number of hydrogen bonds, which break when the H-PDMS is disrupted, and the disrupted parts can be reassembled together by the regeneration of hydrogen bonds when they are retouching together, showing the self-healing function. The mechanical properties of self-healable flexible sensors with different component contents are also shown in Fig. S4 in the supporting information.

The electric conductivity of the sensors before and after self-healing is tested using a Keithley 2400 digital source meter. As shown in Fig. 3(a), when the sensors are cut apart, the resistance immediately rises to infinity, and when the cut-off sensors are reconnected together, the electrical signal returns to the original level instantaneously at the contact moment of two sections with a self-repairing efficiency of 100%. As a metal, conductive method of liquid metal is electronically conductive. Self-repairing ink maintains this nature of liquid metal, which makes electrons transfer occurrence at the moment of liquid metal contact, needless complex conductive network formation. Therefore, when the fractured section is regenerated, the pathway and the electrical signal restore. The mass percent of liquid metal in the ink also affects the resistance of the sensor which shows a decreasing trend as the liquid metal content increases to a certain percentage (25 wt.%) and almost keeps stable (Figs. 3(b) and 3(c)). Since the liquid metal particles (about 2–3 Ω in the resistance) in the ink provide conductive effect, increasing the content of liquid metal in the self-healing ink can make the resistance of the sensor smaller, until the conductive part is close to saturation when the conductivity of liquid metal ink reaches the highest at the content of liquid metal of about 25 wt.%. Additionally, the sensor is also integrated into a circuit consisting of an LED bulb in series (Fig. 3(d)). After cutting off and attaching two damaged interfaces of sensors, the circuit is disconnection and connected again, extinguishing and lightening LED bulb immediately, respectively. This verifies that the sensor has excellent conductive recovery capacity after self-healing.

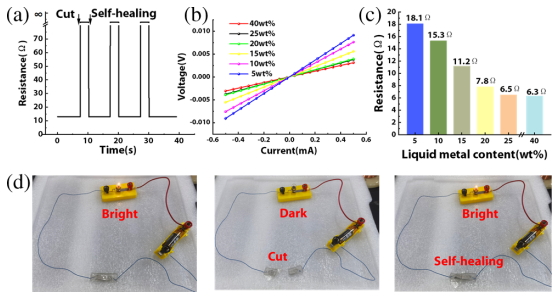

Fig. 3. (a) Electrical properties of the sensor before and after self-healing, (b) effect of mass fractions of liquid metal on sensor resistance, (c) resistance of the sensor with different mass fractions of liquid metal and (d) photographs showing the break-healing process of a sensor with LED bulbs connected in series.

Figure 4 illustrates the sensing characteristics of the sensor during cyclic stretching-releasing tests at different strains (10%, 15%, 30% and 60%) at a stretching speed of 30 mm/min. The variation of $\Delta R/R_0$ of the sensor at different maximum strains during cyclic stretching-releasing process indicates that the maximum value of relative resistance change of the sensor increases with increasing strain and remains stable at the same strain (Fig. 4(a)). This is due to the fact that the increased damage of the conductive network when the strain increase produces a relative larger resistance. The sensor can obtain a reliable sensing signal under different external stimuli at a tensile strain of 25% with tensile speeds of 10, 30 and 50 mm/min, respectively (Fig. 4(b)). The maximum of relative resistance change keeps almost consistent at different stretching rates, which indicates the independence of relative resistance variation of the sensor to the stretching rate. A two-step linear relationship ($R^2 > 98\%$) is obtained between the strain and the relative resistance variation with the sensitivity factor of 0.34 in the strain range from 0% to 32% and 0.81 in the strain range from 32% to 56%, respectively (Fig. 4(c)). The higher sensitivity factor in the second section is attributed to more severely damaged conductive network of the sensor at larger strain. The signals of the sensor

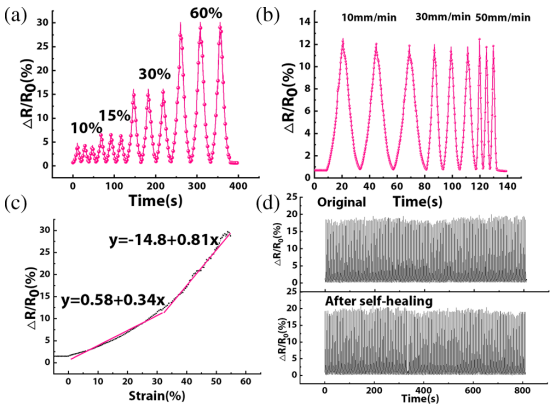

Fig. 4. Sensing performance of sensors (a) at tensile strain of 10%, 15%, 30%, 60% and (b) at different tensile rates at a tensile strain of 25%. (c) linear relations between relative resistance variation and strain and (d) repeatability of sensors before and after self-healing for 24 h.

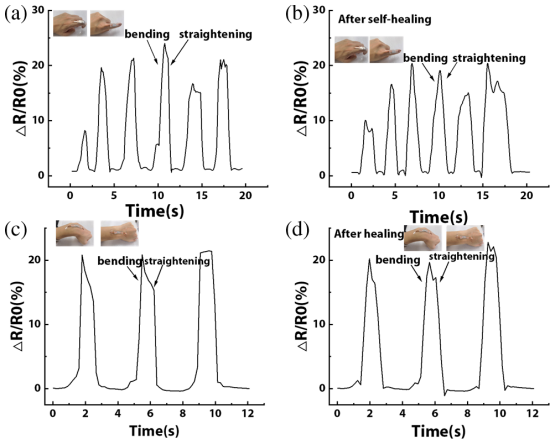

Fig. 5. Relative resistance change of the sensor when the finger is bent-extended (a) before and (b) after the sensor is self-healed for 24 h. Relative resistance change of the sensor when the wrist is bent-extended (c) before and (d) after the sensor is self-healed for 24 h.

before and after self-healing were recorded in multiple cycles of stretching. The sensor displays excellent signal stability and repeatability during 200 tensile cycles at a tensile rate of 100 mm/min and a tensile strain of 30% (Fig. 4(d)).

We further measure the surface roughness and water contact angle of H-PDMS (Fig. S3), and calculate the surface energy of H-PDMS about 22.7 mN/m, which is within the usual surface energy range of PDMS (22–25 mN/m). The surface of H-PDMS is relatively flat with a roughness of 1.966 μm, which is in the same order of magnitude as skin roughness and has comfortable contact with the skin as sensor usage. Considering the satisfactory tensile property, conductivity, strain-sensitive characteristic and reliability, the sensor is used for human motion monitoring. When the sensors are attached to the finger (Fig. 5(a)) and wrist (Fig. 5(c)) of the body through the adhesive tape, the relative resistance variation curves show the corresponding processes of the finger and wrist bending–straightening actions. The same test was then performed after the sensor was destroyed and self-healed for 24 h, and no significant change in the sensor signal can be seen (Figs. 5(b) and 5(d)). This demonstrates the excellent self-healing capability of the sensor and its gratifying ability to monitor human motion. This provides a good idea for the future use of our prepared sensor in the field of medical detection.

In summary, a stretchable, self-healing sensor has been developed by combining PDMS with self-healing properties (H-PDMS) and liquid metal ink. The H-PDMS with a high number of hydrogen bonds can improve the mechanical properties of sensor to withstand tensile stress of up to 0.83 MPa. These hydrogen bonds also grant the sensor robust self-healing properties, with 82% self-healing efficiency after 24 h of self-healing at room temperature. Liquid metal ink is also integrated into the H-PDMS, allowing the sensor to complete 100% electrical signal repair instantly. Additionally, the liquid metal ink provides excellent sensing sensitivity at different strain ranges. Consequently, these wearable strain sensors with a unique combination of self-healing and reliable sensing capabilities make them especially attractive for potential use in robotics, recyclable electronics and other related areas.

Acknowledgments

This work was supported by the National Natural Science Foundation of China (No. 12272351), the Youth Top-notch Talent Project of Zhejiang Ten Thousand Plan of China (No. ZJWR0308010) and the Zhejiang Provincial Natural Science Foundation of China (Nos. LR19E020004 and LR20A020002).

References

1. S. Zhang *et al.*, *iScience* **24**, 103477 (2021).
2. S. Dikhale *et al.*, *IEEE Robot. Autom. Lett.* **7**, 2148 (2022).
3. D. O'Shaughnessy, *Pattern Recognit.* **41**, 2965 (2008).
4. A. S. Miner *et al.*, *NPJ Digit. Med.* **3**, 1 (2020).
5. Z. Amini-Sheshdeh *et al.*, *Sci. Iran.* **22**, 2447 (2015).
6. Y. Zhao *et al.*, *Sensors* **16**, 391 (2016).
7. K. Tang *et al.*, *Sensors* **18**, 1677 (2018).
8. H. Ullah *et al.*, *Biosensors* **12**, 630 (2022).
9. H.-E. Joe *et al.*, *Int. J. Precis. Eng. Manuf., Green Technol.* **5**, 173 (2018).
10. B. Ramachandran *et al.*, *Biomicrofluidics* **16**, 051501 (2022).
11. L. Tang *et al.*, *Materials* **13**, 3947 (2020).
12. T. P. Huynh *et al.*, *Adv. Mater.* **29**, 1604973 (2017).
13. Z. P. Ma *et al.*, *Sens. Actuators A, Phys.* **329**, 18 (2021).
14. D. P. Qi *et al.*, *Adv. Mater.* **33**, 25 (2021).
15. M. P. Wolf *et al.*, *Prog. Polym. Sci.* **83**, 97 (2018).
16. G. Cai *et al.*, *Adv. Sci.* **4**, 1600190 (2017).
17. W.-P. Chen *et al.*, *ACS Appl. Mater. Interfaces* **10**, 1258 (2018).
18. R. L. Parc *et al.*, *Phys. Chem. Chem. Phys.* **21**, 3310 (2019).
19. M. V. D. Schuur *et al.*, *Polymer* **47**, 1091 (2006).
20. K. Sahre *et al.*, *Macromol. Mater. Eng.* **291**, 470 (2006).
21. W. Bai *et al.*, *Angew. Chem. Int. Ed.* **55**, 10707 (2016).